Jurnal Crystal: Publikasi Penelitian Kimia dan Terapannya
Vol. 8, No.1, Page. 213–220, 2026
e-ISSN 2685-7065

SURFACE AREA DRIVEN CRYSTALLINITY CHANGES OF HYDROXYAPATITE DURING SIMULATED BODY FLUID IMMERSION

Agung Prabowo[1*], Ahmad Fadli[2], Heni Sugesti[3], Muh Irwan[1]

[1,] Chemical Engineering Department, Politeknik Negeri Samarinda, Samarinda, 75131, East Kalimantan, Indonesia
[2]Chemical Engineering Department, Engineering Faculty, Universitas Riau, Pekanbaru, 28293, Riau, Indonesia
[3] Chemical Engineering Department, Politeknik Negeri Sriwijaya, Palembang, South Sumatra, Indonesia
[*]E-mail : agungprabowo@polnes.ac.id

Article History
Received: 03 February 2026; Received in Revision: 30 March 2026; Accepted: 31 March 2026

Abstract

The bioactivity of hydroxyapatite (HA) powders is strongly influenced by surface area and crystallinity. This study evaluates the effect of surface area and Ca/P ratio on the bioactivity of HA through immersion in simulated body fluid (SBF) for 3–21 days. Structural and chemical changes were analyzed using XRD, BET, SEM–EDX, and XRF, with bioactivity assessed from XRD peak intensity at 2θ ≈ 30°, degree of crystallinity, Ca/P ratio, calcium ion concentration, and pH variation. The results show that HA maintained its crystal phase during immersion, with the degree of crystallinity varying between 82% and 96%. An initial decrease in crystallinity and peak intensity indicated early HA dissolution, followed by an increase due to apatite layer formation at intermediate immersion times. Prolonged immersion resulted in reduced crystallinity, attributed to calcium depletion and partial re-dissolution. Higher surface area accelerated calcium ion consumption and enhanced apatite formation, confirming improved bioactivity of HA in SBF.

Keywords: Hydroxyapatite, Simulated body fluid (SBF), Crystallinity evolution, X-ray diffraction (XRD), Bioactivity

Abstrak

Bioaktivitas serbuk hidroksiapatit (HA) sangat dipengaruhi oleh luas permukaan dan kristalinitas. Penelitian ini mengevaluasi pengaruh luas permukaan dan rasio Ca/P terhadap bioaktivitas HA melalui perendaman dalam *simulated body fluid* (SBF) selama 3–21 hari. Perubahan struktural dan kimiawi dianalisis menggunakan XRD, BET, SEM–EDX, dan XRF, di mana bioaktivitas dinilai berdasarkan intensitas puncak XRD pada 2θ≈30°, derajat kristalinitas, rasio Ca/P, konsentrasi ion kalsium, serta variasi pH. Hasil penelitian menunjukkan bahwa HA tetap mempertahankan fase kristalnya selama perendaman, dengan derajat kristalinitas bervariasi antara 82% dan 96%. Penurunan awal pada kristalinitas dan intensitas puncak mengindikasikan terjadinya pelarutan (disolusi) awal HA, yang kemudian diikuti oleh peningkatan akibat pembentukan lapisan apatit pada waktu perendaman menengah. Perendaman yang lebih lama mengakibatkan penurunan kristalinitas, yang disebabkan oleh penipisan kalsium dan pelarutan kembali sebagian. Luas permukaan yang lebih tinggi mempercepat konsumsi ion kalsium dan meningkatkan pembentukan apatit, yang mengonfirmasi peningkatan bioaktivitas HA dalam SBF.

Kata Kunci: Hidroksiapatit, *Simulated body fluid* (SBF), Evolusi kristalinitas, Difraksi sinar-X (XRD), Bioaktivitas.

1. Introduction

Bone injuries and degenerative skeletal disorders represent a major global health challenge, driven by aging populations, osteoporosis, traumatic accidents, and degenerative bone diseases (Dong et al., 2021; Kim, Eo, Nguyen, & Kim, 2019; Prabowo et al., 2025). These conditions substantially increase the demand for reliable bone substitute materials capable of restoring both structural integrity and biological function. Although metallic and polymeric implants are widely used in orthopedic and dental applications, their long-term performance remains limited (Chopra, Gulati, & Ivanovski, 2021). Metallic implants often exhibit elastic moduli significantly higher than

that of natural bone, leading to stress shielding and eventual implant failure (Sarraf, Rezvani Ghomi, Alipour, Ramakrishna, & Liana Sukiman, 2022; Zheng, Liu, Ma, Xiao, & Liu, 2018). In contrast, polymeric materials frequently suffer from insufficient mechanical stability, uncontrolled degradation, and unfavorable biological responses in vivo (Chouirfa, Bouloussa, Migonney, & Falentin-Daudré, 2019; Naderi, Zhang, Belgodere, Sunder, & Palardy, 2021). These limitations highlight the need for alternative biomaterials that combine biocompatibility, bioactivity, and structural reliability (Gabay, Ron, Vago, Shirizly, & Aghion, 2021; Remizova, Dzgoeva, Bitarov, & Tingaeva Yu, 2021).

Hydroxyapatite (HA, $Ca_{10}(PO_4)_6(OH)_2$) has emerged as a leading candidate for bone replacement applications due to its close chemical and crystallographic similarity to the mineral phase of human bone (Fiume, Magnaterra, Rahdar, Verné, & Baino, 2021; Fadli etal., 2023). HA is well known for its excellent biocompatibility, osteoconductivity, and ability to form a direct bond with surrounding bone tissue (Fiume et al., 2021; Venkatesan, Anchan, Murugan, Anil, & Kim, 2024). Its bioactivity is closely associated with surface-mediated interactions, where calcium and phosphate ions participate in the nucleation and growth of a bone-like apatite layer (Filip, Surdu, Paduraru, & Andronescu, 2022; Kavasi, Coelho, Platania, Quadros, & Chatzinikolaidou, 2021). Even without altering chemical composition, the surface characteristics of HA strongly influence ion exchange processes and crystallinity evolution in physiological environments (Filip et al., 2022; Kavasi et al., 2021; Venkatesan et al., 2024).

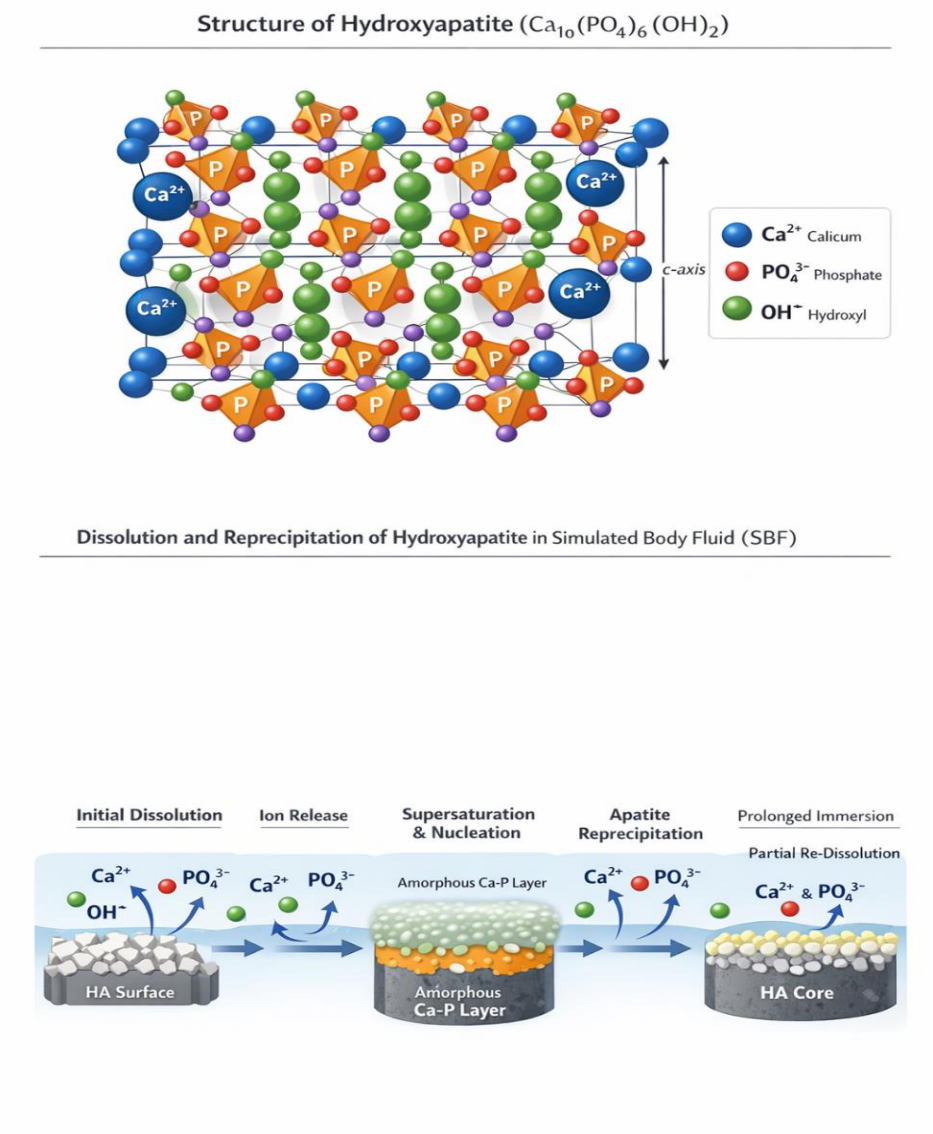

Figure 1. Schematic representation of the crystal/bond structure of hydroxyapatite and a proposed mechanism of dissolution–reprecipitation during SBF immersion

In vitro immersion in simulated body fluid (SBF) is a widely accepted method for evaluating the bioactivity of HA (Hussin, Abdullah, Idris, & Wahap, 2022). The formation of an apatite layer during SBF immersion is considered a reliable indicator of in vivo bone-bonding potential. However, many previous studies primarily rely on qualitative surface observations, such as morphological changes detected by microscopy, to assess bioactivity (Pratama et al., 2025). Quantitative evaluation of crystallinity evolution and diffraction peak intensity during immersion—parameters that directly reflect structural reorganization at the atomic scale—remains relatively underexplored (da Silva Brum et al., 2019). In particular, the dynamic relationship between dissolution, reprecipitation, and crystallinity changes of HA during prolonged SBF exposure has not been sufficiently clarified (da Silva Brum et al., 2019).

Table 1. Chemical and Physical Properties of Hydroxyapatite (HA)

Property	**Description / Value**
Chemical formula	$Ca_{10}(PO_4)_6(OH)_2$
Molecular weight	1004.64 g/mol
Ca/P molar ratio	1.67 (stoichiometric HA)
Crystal structure	Hexagonal (space group: $P6_3/m$)
Lattice parameters	a ≈ 9.42 Å, c ≈ 6.88 Å
Density	~3.16 g/cm³

Crystallinity plays a critical role in determining the biological performance of HA. Variations in crystallinity influence solubility, ion release behavior, and the stability of the apatite layer formed on the material surface (da Silva Brum et al., 2019). During SBF immersion, HA may undergo an initial dissolution stage, followed by reprecipitation and growth of a new apatite layer, leading to non-monotonic changes in crystallinity (Pratama et al., 2025). These processes can be effectively monitored through changes in X-ray diffraction (XRD) peak intensity, particularly at characteristic HA reflections around 2θ ≈ 30°, which are sensitive to both crystal ordering and crystallite growth (Ofudje, Adeogun, Idowu, & Kareem, 2019).

In this study, the bioactivity of hydroxyapatite powder with a single, well-defined surface area of 35.27 m²/g is investigated through systematic immersion in SBF for 3, 7, 14, and 21 days. Structural evolution is quantitatively analyzed using X-ray diffraction, with emphasis on changes in diffraction peak intensity and degree of crystallinity. These results are correlated with Ca/P ratio variation and calcium ion depletion in the SBF solution to elucidate the mechanisms governing apatite layer formation (Battafarano et al., 2021). By focusing on crystallinity evolution rather than surface area variation, this work provides clear mechanistic insight into the bioactive behavior of HA in physiological-like environments and contributes to the rational design of HA-based biomaterials for bone regeneration and implant applications (Xing, Zhong, Chen, & Liu, 2023; Y. Zhang, Poon, Masonsong, Ramaswamy, & Singh, 2023). This study introduces a quantitative crystallinity-based framework to evaluate hydroxyapatite bioactivity, revealing a non-monotonic structural evolution governed by dissolution–reprecipitation mechanisms during SBF immersion.

2. Methodology

2.1 Materials

Hydroxyapatite (HA) powder used in this study was synthesized via an optimized precipitation method, followed by controlled aging and calcination at 600 °C. The obtained HA powder exhibited a specific surface area of 35.27 m²/g and a Ca/P molar ratio of 1.67, corresponding to stoichiometric hydroxyapatite. This material was selected to represent a porous HA system with surface characteristics favorable for bioactivity evaluation. Simulated body fluid (SBF) was prepared using analytical-grade reagents, including sodium chloride (NaCl), sodium bicarbonate ($NaHCO_3$), potassium chloride (KCl), dipotassium hydrogen phosphate trihydrate ($K_2HPO_4 \cdot 3H_2O$), magnesium chloride hexahydrate ($MgCl_2 \cdot 6H_2O$), calcium chloride ($CaCl_2$), sodium sulfate (Na_2SO_4), tris(hydroxymethyl)aminomethane (Tris), and hydrochloric acid (HCl). All chemicals were purchased from Merck (Germany) and used as received without further purification. Sterile distilled water was used throughout the experiment.

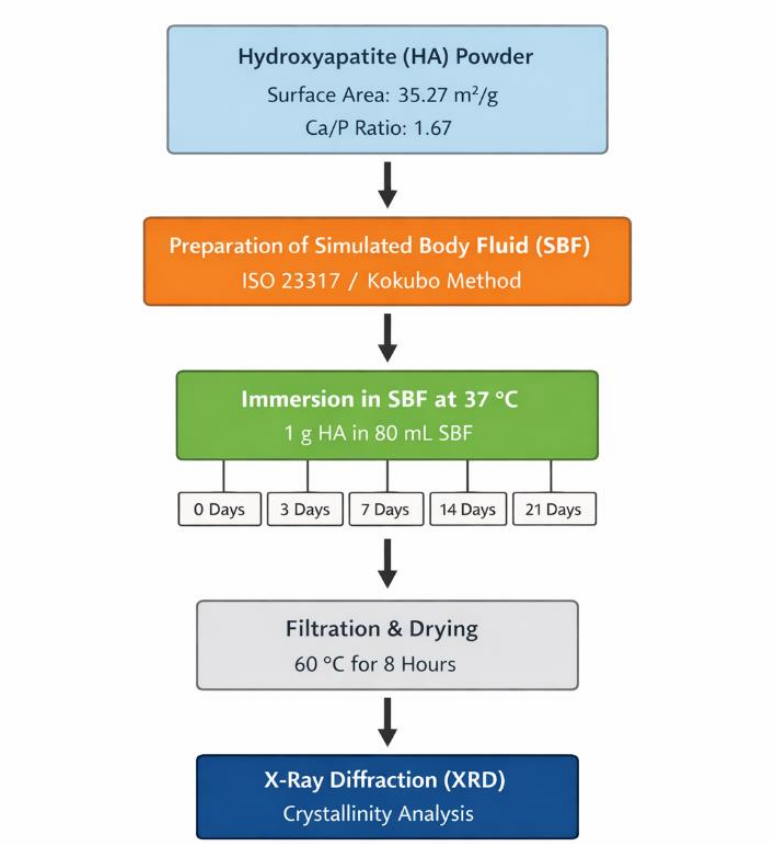

Figure 2. Experimental Flowchart of HA Immersion in Simulated Body Fluid

2.2 Preparation of Simulated Body Fluid (SBF)

The simulated body fluid (SBF) solution was prepared in accordance with ISO/FDIS 23317 and the method described by Kokubo and Takadama, ensuring ionic concentrations comparable to those of human blood plasma. The reagent composition for preparing 1 L of SBF is summarized in Table 2. The pH of the solution was adjusted to 7.40 ± 0.02 at 37 °C using 1.0 M HCl. Fresh SBF solution was prepared prior to each immersion experiment to ensure consistency and reliability.

Table 2. Reagent composition for the preparation of 1 L of SBF.

No	Reagent	Chemical Name	Quantity
1	NaCl	Sodium chloride	8.035 g
2	$NaHCO_3$	Sodium bicarbonate	0.355 g
3	KCl	Potassium chloride	0.225 g
4	$K_2HPO_4 \cdot 3H_2O$	Dipotassium hydrogen phosphate trihydrate	0.231 g
5	$MgCl_2 \cdot 6H_2O$	Magnesium chloride hexahydrate	0.311 g
6	HCl (1.0 M)	Hydrochloric acid (1.0 M)	39 mL
7	$CaCl_2$	Calcium chloride	0.292 g
8	Na_2SO_4	Sodium sulfate	0.072 g
9	Tris	Tris(hydroxymethyl)aminomethane	6.118 g
10	HCl (1.0 M)	Hydrochloric acid (1.0 M)	0–5 mL

2.3 In Vitro SBF Immersion Test

The in vitro bioactivity of the HA powder was evaluated by immersion in SBF under physiological conditions. One gram (1 g) of HA powder was immersed in 80 mL of SBF in sealed polyethylene containers. The immersion was conducted at a constant temperature of 37 ± 1 °C to simulate the human body environment. The immersion periods were set at 0 (before immersion), 3, 7, 14, and 21 days. At each designated time interval, the HA powder was carefully separated from the SBF

solution by filtration. The recovered powders were gently rinsed with distilled water to remove residual ions and dried in an oven at 60 °C for 8 h prior to characterization. This procedure ensured that the observed structural changes originated from the interaction between HA and SBF rather than from residual solution effects.

2.4 X-ray Diffraction (XRD) Analysis

X-ray diffraction (XRD) analysis was employed as the primary characterization technique to investigate the structural evolution and crystallinity changes of HA before and after immersion in SBF. Diffraction patterns were recorded using Cu Kα radiation over a suitable 2θ range. Particular emphasis was placed on the main diffraction peak of hydroxyapatite at 2θ ≈ 30°, which is highly sensitive to variations in crystal order and apatite formation. The degree of crystallinity was determined from the XRD data using peak intensity analysis. Changes in diffraction peak intensity and crystallinity as a function of immersion time were used to evaluate the bioactive response of HA, reflecting the balance between initial surface dissolution and subsequent reprecipitation of apatite induced by interaction with SBF

3. Results and Discussion

For the hydroxyapatite (HA) sample with a specific surface area of 35.27 m²/g and a Ca/P ratio of 1.67, the effect of immersion time in simulated body fluid (SBF) on crystallinity evolution can be quantitatively evaluated through the combined analysis of XRD patterns (Figure 2) and the corresponding degree of crystallinity values (Table 3). The XRD diffraction patterns at all immersion times exhibit characteristic HA reflections without the appearance of secondary phases, indicating that the HA crystal structure remains stable throughout the immersion process (Figure 2a–e).

Table 3. Degree of Crystallinity of HA Powders

Ca/P	Surface Area (m²/g)	Degree of Crystallinity (%)				
		0 days	3 days	7 days	14 days	21 days
1.67	35.27	96.33	84.53	91.73	91.41	82.11

Prior to immersion (0 days), the HA sample shows a high degree of crystallinity of 96.33% (Table 2), accompanied by a pronounced diffraction peak at 2θ ≈ 30° with an intensity of 273.37 cts (Figure 3a). This high peak intensity reflects a well-ordered crystalline structure with minimal lattice distortion, providing a reliable baseline for assessing structural changes induced by SBF exposure (Abd-Aljbar, Alattar, Khalaf, & Odah, 2025; Ogunleye et al., 2025; Yang, Willhammar, Xu, Zou, & Huang, 2022).

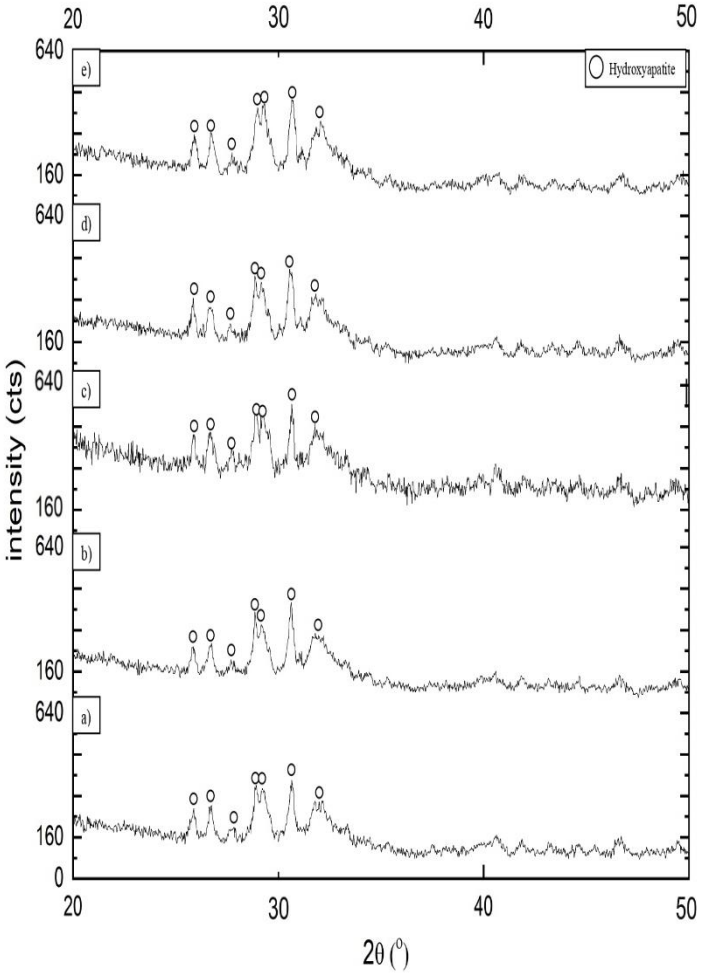

Figure 3. X-ray diffraction (XRD) patterns of hydroxyapatite (HA) with a specific surface area of 35.27 m²/g and a Ca/P ratio of 1.67 after immersion in simulated body fluid (SBF) for different durations: (a) 0 days, (b) 3 days, (c) 7 days, (d) 14 days, and (e) 21 days.

After 3 days of immersion, the intensity of the main diffraction peak at 2θ ≈ 30° decreases to 182.33 cts (Figure 3b), consistent with a reduction in crystallinity to 84.53% as summarized in Table 2. This decrease indicates the occurrence of initial surface dissolution of HA crystallites, particularly at energetically unfavorable surface sites. The relatively high surface area of 35.27 m²/g enhances the interaction between HA and SBF, accelerating the release of Ca^{2+} and PO_4^{3-} ions and leading to a temporary reduction in crystal ordering (Costentin, Drouet, Salles, & Sarda, 2022; Moosakazemi, Sahraei, Bouchard, & Larachi, 2025; L. Zhang et al., 2024).

With increasing immersion time to 7 days, a significant increase in diffraction peak intensity is observed, reaching 402.35 cts at 2θ ≈ 30° (Figure 3c). Correspondingly, the degree of crystallinity increases to 91.73% (Table 2). This behavior suggests that reprecipitation and growth of an apatites layer dominate at this stage. Calcium and phosphate ions from the SBF are adsorbed onto the HA surface, promoting nucleation and growth of a more ordered apatite phase, which is reflected in the enhanced peak intensity and increased crystallinity.

Upon extending the immersion period to 14 and 21 days, the XRD patterns (Figure 3d–e) show a gradual decrease in peak intensity, with the intensity at 2θ ≈ 30° declining to 300.04 cts after 21 days, accompanied by a reduction in crystallinity to 82.11% as reported in Table 3. This trend indicates that during prolonged immersion, a dissolution–precipitation imbalance develops. Continuous consumption of Ca^{2+} ions for apatite formation results in partial calcium depletion within the HA lattice, while the newly formed apatite layer becomes less ordered or partially amorphous, contributing to the observed decrease in crystallinity. Overall, the fluctuating diffraction peak intensity observed in Figure 2, together with the non-monotonic changes in

crystallinity summarized in Table 2, clearly demonstrate the dynamic nature of HA–SBF interactions. The initial decrease, subsequent increase, and final reduction in crystallinity correspond to early dissolution, optimal apatite layer formation, and partial degradation during long-term immersion, respectively. These results confirm that hydroxyapatite with a surface area of 35.27 m^2/g exhibits pronounced bioactivity, as evidenced by its ability to induce apatite layer formation under physiological-like conditions.

4. Conclusion

This study demonstrates that the bioactivity of hydroxyapatite (HA) with a specific surface area of 35.27 m^2/g is governed by a dynamic interplay between dissolution and reprecipitation processes during immersion in simulated body fluid (SBF). The HA structure remains phase-stable throughout the immersion period, while its crystallinity exhibits a clear non-monotonic evolution. An initial decrease in crystallinity confirms early-stage surface dissolution, followed by a significant increase at intermediate immersion times due to the formation of a newly precipitated apatite layer. Prolonged immersion leads to a subsequent reduction in crystallinity, attributed to calcium depletion and partial re-dissolution of the formed layer. These findings highlight that crystallinity evolution, particularly as reflected by XRD peak intensity at $2\theta \approx 30°$, provides a sensitive and quantitative indicator of HA bioactivity. The relatively high surface area accelerates ion exchange and promotes apatite nucleation, confirming its critical role in enhancing bioactive performance. Overall, this work provides clear mechanistic insight into HA–SBF interactions and underscores the importance of controlling surface characteristics to optimize the design of hydroxyapatite-based biomaterials for bone regeneration and implant applications.

References

Abd-Aljbar, A. A., Alattar, A. M., Khalaf, M. K., & Odah, J. F. (2025). Influence of irradiation on the corrosion resistance of medical stainless-steel alloys coated with nickel-titanium layers. *Radiation Physics and Chemistry*, 113397.

Battafarano, G., Rossi, M., De Martino, V., Marampon, F., Borro, L., Secinaro, A., & Del Fattore, A. (2021). Strategies for bone regeneration: from graft to tissue engineering. *International journal of molecular sciences, 22*(3), 1128.

Chopra, D., Gulati, K., & Ivanovski, S. o. (2021). Micro+ nano: conserving the gold standard microroughness to nanoengineer zirconium dental implants. *ACS Biomaterials Science & Engineering, 7*(7), 3069-3074.

Chouirfa, H., Bouloussa, H., Migonney, V., & Falentin-Daudré, C. (2019). Review of titanium surface modification techniques and coatings for antibacterial applications. *Acta biomaterialia, 83*, 37-54.

Costentin, G., Drouet, C., Salles, F., & Sarda, S. (2022). Structure and Surface Study of Hydroxyapatite-Based Materials: Experimental and Computational Approaches. *Design and Applications of Hydroxyapatite-Based Catalysts*, 73-140.

da Silva Brum, I., de Carvalho, J. J., da Silva Pires, J. L., de Carvalho, M. A. A., Dos Santos, L. B. F., & Elias, C. N. (2019). Nanosized hydroxyapatite and β-tricalcium phosphate composite: Physico-chemical, cytotoxicity, morphological properties and in vivo trial. *Scientific Reports, 9*(1), 19602.

Dong, Z., Ke, X., Tang, S., Wu, S., Wu, W., Chen, X., . . . Li, J. (2021). A stable cell membrane-based coating with antibiofouling and macrophage immunoregulatory properties for implants at the macroscopic level. *Chemistry of Materials, 33*(20), 7994-8006.

Fadli, A., Prabowo, A., Utama, Panca setia, Aziz, Y., & Heltina, D. (2023). SIGNIFICANCE OF THE PCL CONCENTRATION ON THE ELECTROCHEMICAL AND MECHANICAL PERFORMANCE OF A PCL/HA COATING ON SS 316L. *Ceramics–Silikáty*, *67*(4), 551-561.

Filip, D. G., Surdu, V.-A., Paduraru, A. V., & Andronescu, E. (2022). Current development in biomaterials—hydroxyapatite and bioglass for applications in biomedical field: a review. *Journal of Functional Biomaterials, 13*(4), 248.

Fiume, E., Magnaterra, G., Rahdar, A., Verné, E., & Baino, F. (2021). Hydroxyapatite for biomedical applications: A short overview. *Ceramics, 4*(4), 542-563.

Gabay, N., Ron, T., Vago, R., Shirizly, A., & Aghion, E. (2021). Evaluating the Prospects of Ti-Base Lattice Infiltrated with Biodegradable Zn–2% Fe Alloy as a Structural Material for Osseointegrated Implants—In Vitro Study. *Materials, 14*(16), 4682.

Hussin, M. S. F., Abdullah, H. Z., Idris, M. I., & Wahap, M. A. A. (2022). Extraction of natural hydroxyapatite for biomedical applications—A review. *Heliyon, 8*(8).

Kavasi, R.-M., Coelho, C. C., Platania, V., Quadros, P. A., & Chatzinikolaidou, M. (2021). In vitro biocompatibility assessment of nano-hydroxyapatite. *Nanomaterials, 11*(5), 1152.

Kim, K. T., Eo, M. Y., Nguyen, T. T. H., & Kim, S. M. (2019). General review of titanium toxicity. *International journal of implant dentistry, 5*(1), 10.

Moosakazemi, F., Sahraei, A. A., Bouchard, J., & Larachi, F. (2025). Termination-dependent surface chemistry of pyrochlore flotation: stability, hydration, and collector adsorption. *Minerals Engineering, 234*, 109728.

Naderi, A., Zhang, B., Belgodere, J. A., Sunder, K., & Palardy, G. (2021). Improved biocompatible, flexible mesh composites for implant applications via hydroxyapatite coating with potential for 3-dimensional extracellular matrix network and bone regeneration. *ACS applied materials & interfaces, 13*(23), 26824-26840.

Ofudje, E. A., Adeogun, A. I., Idowu, M. A., & Kareem, S. O. (2019). Synthesis and characterization of Zn-Doped hydroxyapatite: scaffold application, antibacterial and bioactivity studies. *Heliyon, 5*(5).

Ogunleye, A. M., Lee, H., Awwal, A. M., Kim, G., Kim, H., Choi, Y., & Park, J. (2025). Inherent Lattice Distortion Engineering via Magnetic Field for High-Quality Strained MAPbI3 Perovskite Single Crystals. *Advanced Materials Interfaces, 12*(9), 2400781.

Prabowo, A., Fadli, A., Sugesti, H., Irwan, M., Oko, S., & Mahardika, G. B. (2025). ADHESIVE BEHAVIOR OF POLYCAPROLACTONE/HYDROXYAPATITE COATINGS ON 316L STAINLESS STEEL: A DESIGN OF EXPERIMENTS APPROACH. *Jurnal Crystal: Publikasi Penelitian Kimia dan Terapannya*, *7*(2), 209-220.

Pratama, Y. A., Marhaeny, H. D., Deapsari, F., Budiatin, A. S., Rahmadi, M., Miatmoko, A., . . . Khotib, J. (2025). Development of Hydroxyapatite as a Bone Implant Biomaterial for Triggering Osteogenesis. *European Journal of Dentistry*.

Remizova, A., Dzgoeva, M. G., Bitarov, P., & Tingaeva Yu, I. (2021). Personalized approach to the choice of orthopedic design depending on the predicted stability of implants. *Медицинский вестник Северного Кавказа, 16*(2), 173-175.

Sarraf, M., Rezvani Ghomi, E., Alipour, S., Ramakrishna, S., & Liana Sukiman, N. (2022). A state-of-the-art review of the fabrication and characteristics of titanium and its alloys for biomedical applications. *Bio-design and Manufacturing, 5*(2), 371-395.

Venkatesan, J., Anchan, R. V., Murugan, S. S., Anil, S., & Kim, S.-K. (2024). Natural hydroxyapatite-based nanobiocomposites and their biomaterials-to-cell interaction for bone tissue engineering. *Discover Nano, 19*(1), 169.

Xing, Y., Zhong, X., Chen, Z., & Liu, Q. (2023). Optimized osteogenesis of biological hydroxyapatite-based bone grafting materials by ion doping and osteoimmunomodulation. *Bio-Medical Materials and Engineering, 34*(3), 195-213.

Yang, T., Willhammar, T., Xu, H., Zou, X., & Huang, Z. (2022). Single-crystal structure determination of nanosized metal–organic frameworks by three-dimensional electron diffraction. *Nature protocols, 17*(10), 2389-2413.

Zhang, L., Liang, X., Chen, J., Kang, Z., Ye, J., & Xie, D. (2024). Evolution of phase, morphology, physicochemical properties, and biological properties of HA ceramic with the increase of crystallinity. *Ceramics International, 50*(18), 33153-33163.

Zhang, Y., Poon, K., Masonsong, G. S. P., Ramaswamy, Y., & Singh, G. (2023). Sustainable nanomaterials for biomedical applications. *Pharmaceutics, 15*(3), 922.

Zheng, Y., Liu, L., Ma, Y., Xiao, L., & Liu, Y. (2018). Enhanced osteoblasts responses to surface-sulfonated polyetheretherketone via a single-step ultraviolet-initiated graft polymerization. *Industrial & Engineering Chemistry Research, 57*(31), 10403-10410.